Metabolomics (2008) 4:297–311
DOI 10.1007/s11306-008-0120-8

ORIGINAL ARTICLE

Rapid analysis of pharmaceuticals and excreted xenobiotic and endogenous metabolites with atmospheric pressure infrared MALDI mass spectrometry

Bindesh Shrestha · Yue Li · Akos Vertes

Received: 9 March 2008 / Accepted: 9 July 2008 / Published online: 20 July 2008

Abstract Atmospheric pressure (AP) infrared (IR) matrix-assisted laser desorption/ionization (MALDI) mass spectrometry (MS) was demonstrated for the rapid direct analysis of pharmaceuticals, and excreted human metabolites. More than 50 metabolites and excreted xenobiotics were directly identified in urine samples with high throughput. As the water content of the sample was serving as the matrix, AP IR-MALDI showed no background interference in the low mass range. The structure of targeted ions was elucidated from their fragmentation pattern using collision activated dissociation. The detection limit for pseudoephedrine was found to be in the sub-femtomole range and the semi-quantitative nature of the technique was tentatively demonstrated for a metabolite, fructose, by using a homologous internal standard, sucrose. A potential application of AP IR-MALDI for intestinal permeability studies was also explored using polyethylene glycol.

Keywords Mass spectrometry · Pharmaceuticals · Human metabolomics · Metabolites · Matrix-assisted laser desorption ionization · MALDI · Atmospheric pressure MALDI · Infrared MALDI · Intestinal permeability

Abbreviations

AP	Atmospheric pressure
IR	Infrared
MALDI	Matrix-assisted laser desorption/ionization (MALDI)
MS	Mass spectrometry
DESI	Desorption electrospray ionization
DART	Direct analysis in real time
DAPCI	Desorption atmospheric pressure chemical ionization
LAESI	Laser ablation electrospray ionization
DIOS	Desorption ionization on silicon
LISMA	Laser-induced silicon microcolumn arrays
CAD	Collision activated dissociation
LOD	Limit of detection
m/z	Mass-to-charge ratio

B. Shrestha · Y. Li · A. Vertes (✉)
Department of Chemistry, W. M. Keck Institute for Proteomics Technology and Applications, George Washington University, Washington, DC 20052, USA
e-mail: vertes@gwu.edu

1 Introduction

Advances in combinatorial chemistry have lead to a remarkable increase in the synthesis of drug candidates. As a result high-throughput analytical techniques are needed for their detection and structural identification during synthesis and in biological activity assessment (Triolo et al. 2001). Mass spectrometry is a well established tool for the analysis of xenobiotic and endogenous metabolites (Dettmer et al. 2007; Glassbrook et al. 2000; Nicholson et al. 2002; Siuzdak 1994). Many other non-mass spectrometric techniques, such as infrared spectrometry (Blanco et al. 1998; Guimarães et al. 2006; MacDonald and Prebble 1993), Raman spectroscopy (Strachan et al. 2007), terahertz imaging (Kawase et al. 2003), fluorescence spectroscopy (Moreira et al. 2005) and nuclear magnetic resonance (Balchin et al. 2005; Maher et al. 2007; Popchapsky and Popchapsky 2001), provide useful and complementary information on their chemical composition. Mass spectrometry gives unique insights into metabolism due to its high sensitivity and the ability to selectively identify these molecules through fragmentation studies.

The detection of metabolites for medical diagnosis and for clinical or forensic toxicology is dominated by hyphenated approaches (Bowers 1997; Dettmer et al. 2007; Papac and Shahrokh 2001), such as gas chromatography-MS (Wolthers and Kraan 1999), liquid chromatography-MS (Kostiainen et al. 2003; Niessen 1999) and capillary electrophoresis-MS (Smyth and Rodriguez 2007). The conventional mass spectrometric methods for drug and metabolite studies require extensive sample preparation and/or extended analysis time.

Sample preparation and analysis time can be reduced by using ambient ion sources. A variety of recently introduced methods, including desorption electrospray ionization (DESI) (Chen et al. 2005; Kauppila et al. 2006; Leuthold et al. 2006; Takats et al. 2004), direct analysis in real time (DART) (Cody et al. 2005), desorption atmospheric pressure chemical ionization (DAPCI) (Takats et al. 2005), extractive electrospray ionization (EESI) (Chen et al. 2006b; Chen et al. 2007), plasma-assisted desorption/ionization (PADI) (Ratcliffe et al. 2007), and laser ablation electrospray ionization (LAESI) (Nemes and Vertes 2007), have demonstrated the capability of ambient analysis of complex samples without extensive sample preparation. A recent comparative study of DESI, DART, and DAPCI has shown that the three methods provide complementary information for a range of pharmaceuticals (Williams et al. 2006).

Since its inception in 1988, matrix-assisted laser desorption/ionization (MALDI) mass spectrometry (MS) has been used as a tool for analysis of large biomolecules and synthetic polymers (Karas and Hillenkamp 1988; Tanaka et al. 1988). The application of MALDI MS for low mass compounds of biological interest (Duncan et al. 1993; Lidgard and Duncan 1995), such as carbohydrates, amino acids etc., has been recently reviewed (Cohen and Gusev 2002). The use of MALDI for the analysis of small molecules is primarily limited by often overwhelming background interference from the matrix molecules in the low mass region. To overcome this limitation, Siuzdak and coworkers introduced a matrix-free approach called desorption ionization on silicon (DIOS) (Wei et al. 1999). DIOS (Go et al. 2003) and other matrix-free laser ionization methods, e.g., laser-induced silicon micro-column arrays (LISMA) (Chen and Vertes 2006), have demonstrated excellent sensitivity for small molecule analysis. With these methods, however, the direct analysis of biological fluids has not been demonstrated.

At mid-infrared laser wavelengths (2.94 μm), a non-interfering MALDI matrix, such as ice or water, can also be used to analyze proteins (Berkenkamp et al. 1996) and small metabolites (Li et al. 2008). As most cells and tissues contain 60–90% water, it is an attractive matrix to study biological samples. Many pharmaceutical formulations (e.g., syrups, ointments and gels) and mother liquors in pharmaceutical synthesis also contain significant amounts of water. Atmospheric pressure (AP) IR-MALDI could enable the rapid direct analysis of these samples with little or no sample preparation (Laiko et al. 2000; Laiko et al. 2002).

Soft laser desorption ionization techniques use a focused laser beam to ionize the sample. This local analysis capability enables chemical imaging of biological tissues to spatially map the distribution of pharmaceutical compounds in various tissues (Bunch et al. 2004; Hsieh et al. 2006; Reyzer et al. 2003). In addition to providing an attractive alternative for imaging the distribution of pharmaceuticals and their metabolites in tissue without the need to apply an external matrix, AP IR-MALDI could also enable high-throughput analysis of samples in a multi-well plate under ambient conditions. We have recently described the utility of AP IR-MALDI for the analysis and imaging of plant metabolites directly from tissue samples (Li et al. 2007, 2008). The present study explores the use of AP IR-MALDI for the analysis of selected pharmaceuticals in their commercial formulations, and the related metabolites in human urine.

2 Materials and methods

2.1 AP IR-MALDI instrumentation

All the experiments were carried out with an orthogonal acceleration time-of-flight mass spectrometer, Q-TOF Premier (Waters Co., Milford, MA), utilizing a custom made atmospheric pressure MALDI interface described elsewhere (Li et al. 2007, 2008). The sample deposited on a stainless steel target was ionized by a Nd:YAG laser-driven optical parametric oscillator (Opotek, Carlsbad, CA) running at 2.94 μm wavelength, 10 Hz repetition rate, and 5 ns pulse width. The laser beam was steered and aligned by SiO protected gold mirrors (Thorlabs, Newton, NJ) with >97.5% reflectivity to a plano-convex calcium fluoride lens with 50 mm focal length (Infrared Optical Products, Farmingdale, NY). The laser beam was focused with the lens to the target surface at an approximately 45° incidence angle producing an elliptical laser spot with $\sim 250 \times 650$ μm^2 dimensions. The average pulse energy was 240 ± 10 μJ, which corresponded to a fluence of 0.20 ± 0.02 J/cm^2. The target was placed on a 3-axis translation stage for sample positioning and geometry optimization. The distance between the mass spectrometer inlet orifice and the target surface was set to ~ 2 mm to maximize the ion signal intensity without producing an electrical breakdown or adversely effecting the focusing. A pulsed voltage of $\pm$ 3.0 kV was applied to the target in order to improve the ion collection efficiency. In this technique, known as pulsed

dynamic focusing, the high voltage on the target is reduced to zero after ~10 μs as expanding plume approaches the inlet orifice of the mass spectrometer. This results in the optimal combination of electric field and aerodynamic flow for ion collection (Tan et al. 2004). Typically, the mass spectrometer orifice was heated to 50°C and kept at constant −50 V or 50 V potential for positive or negative ions, respectively. Prior to the analyses, the mass spectrometer was calibrated with sodium iodide cluster ions from 0.01 M solution. Additionally internal calibration was performed in each analysis based on the *m/z* values of certain known metabolites. The fragments for tandem mass spectrometry were generated by collision activated dissociation (CAD) with argon gas using typical collision energies between 15 and 30 eV, and 4×10^{-3} mbar pressure.

2.2 Materials and sample preparation

Pure active ingredients (pseudoephedrine, ketoprofen, loratadine, melatonin, naphthoquinone, propranolol, and verapamil) of the formulated drugs were purchased from Sigma-Aldrich (St. Louis, MO). All reagents were at least 98% pure and they were used without the further purification. Over-the-counter tablets (ibuprofen), syrup (acetaminophen, dextromethorphan, doxylamine, and pseudoephedrine), gelatin capsule (acetaminophen, dextromethorphan, guaifenesin, and pseudoephedrine), and powder (aspirin, caffeine, and salicylamide) drugs were obtained from a local pharmacy (Washington, D.C.). The concentrations of the active ingredients among the formulations varied, typically anywhere from 1 to 100 mM. When needed deionized water from a D4631 E-pure system (Barnstead, Dubuque, IA) was used for the sample preparations. Only a few microliters or a few milligrams of the samples were placed on the stainless steel target for analysis. Medications in solid form (e.g., tablets or powders) were analyzed either by mounting a fragment on the target with a double sided conductive tape or applied as an aqueous solution. In order to prevent spectral interferences from the conductive tape, the solid samples were kept at least a few hundred micrometers thick. The target was cleaned with ~50% ethanol/water mixture between analyses to avoid any cross-contamination or carryover.

Sample preparation in most cases was not necessary. For coated tablets and capsules, prior to analysis by mass spectrometry the inside contents had to be exposed. Multiple laser shots at a single spot were utilized to ablate the coating, and provided mass spectra for the different layers of the tablet. Alternatively the coating was removed by physical abrasion, which only added a few seconds of analysis time. Fresh urine sample was obtained from a presumably healthy Asian male volunteer in his mid-20 s with normal medical history. There were no dietary restrictions except for total abstinence from alcoholic beverages, and smoking 24 h prior to the administration of the medicine. The urine samples were collected at various times before and after (2.5 h, and 24 h) the single-dose oral administration of a gelatin capsule containing the following active ingredients; acetaminophen (250 mg), dextromethorphan (10 mg), guaifenesin (100 mg), and pseudoephedrine (10 mg). For the analysis of metabolites in urine, two parallel trials were performed on the same individual within two weeks from each other. The presented *m/z* values for the metabolites in urine were obtained from typical mass spectra averaged over two hundred scans from a single sample.

3 Results and discussion

3.1 Sensitivity and quantitative analysis

Initially AP MALDI was considered less sensitive than its vacuum counterpart due to the inefficiency of the ion collection, and transportation through the atmospheric interface. Recently attomole range sensitivity has been reported for ultraviolet AP MALDI using an electrospray matrix deposition technique (Wei et al. 2004). The same experimental setup gave low femtomole range sensitivity when the conventional dried droplet method was used for matrix deposition. To evaluate the detection limit of our AP IR-MALDI setup for small molecules, solutions of pseudoephedrine (molecular weight: 165.1153 g/mol) were prepared in deionized water containing 0.1% trifluoroacetic acid. At the limit of detection (LOD), defined as signal-to-noise ratio greater than 3, the total amount of pseudoephedrine deposited on a cold finger target was 1 pmol. For a single analyzed spot on the target, the LOD was calculated to be 230 amol, which approached the performance of vacuum MALDI ion sources. Figure 1 shows the signal-to-noise ratio for the pseudoephedrine solutions as a function of analyte amount in the probed area. The inset in the figure presents a typical mass spectrum of pseudoephedrine for 230 amol analyte.

Generally quantitative analysis by MALDI is complicated by variable signal intensity due to laser pulse energy fluctuations, and as a consequence of inhomogeneous analyte distribution in the sample. Above the ion generation threshold, the signal amplitude of the analyte as a function of laser irradiance follows a power low relationship with ~6 in the exponent (Ens et al. 1991). Thus small variations in the laser output result in disproportionally magnified MALDI signal variations. Structural isomer or stable isotope analogues as internal standards can be used to factor out this variability and enhance quantitation (Duncan et al. 1993; Tang et al. 1993).

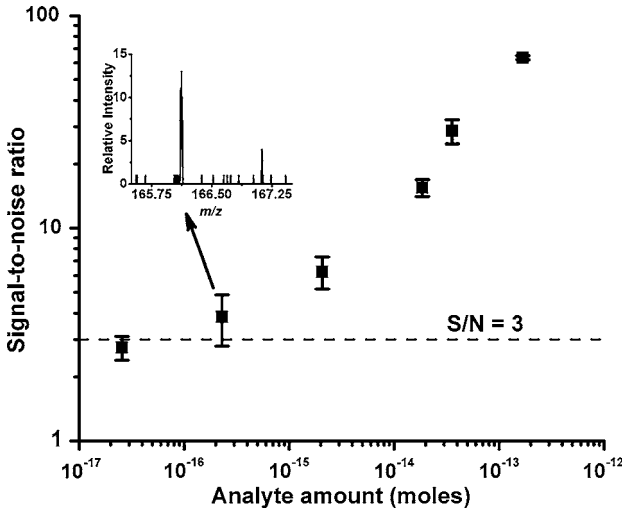

Fig. 1 Signal-to-noise ratio for pseudoephedrine ions as a function of the analyte amount in the ablated volume. The limit of detection (LOD) of AP IR-MALDI for aqueous solutions of pseudoephedrine was in the sub-femtomole range. The inset shows the mass spectrum of pseudoephedrine at its detection limit

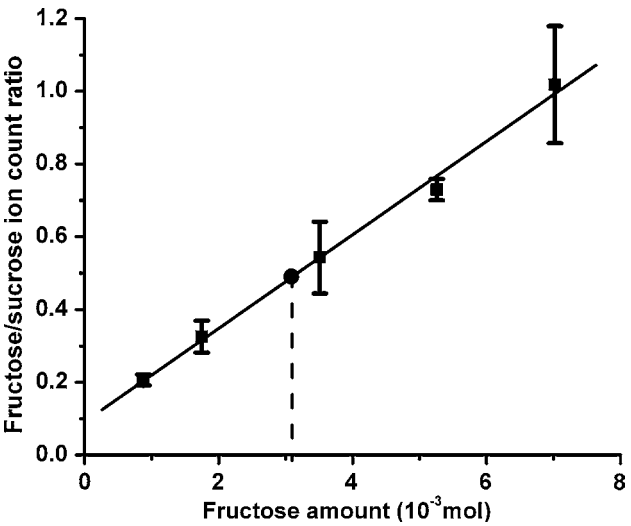

Fig. 2 Sodiated sucrose ion was used as an internal standard to construct a calibration curve for fructose in water using AP IR-MALDI. The amount of fructose in a sample was determined with ~12% accuracy (solid circle)

To gauge the dynamic range of AP IR-MALDI, samples with different amounts of fructose were dissolved and analyzed in an aqueous sucrose/Na^+ solution. As shown in Fig. 2, the ratio of sodiated fructose to sucrose ion counts increased linearly with increasing the amount of fructose in the solution. Thirty mass spectra were averaged to improve the signal-to-noise ratio. Using Fig. 2 as a calibration curve to estimate the amount of fructose present in a test sample (denoted with a solid circle in Fig. 2) yielded ~12% accuracy. This preliminary result is encouraging, but extended studies on multiple analytes with variety of interferences and systems are needed to establish the quantitation capabilities of AP IR-MALDI.

The effect of the various ion source parameters, such as the laser fluence, target voltage, axial and radial position of the laser focal spot versus the inlet orifice, and the orifice temperature, on the ion yield was studied to establish optimum conditions (Li et al. 2007, 2008).

The laser fluence dependence of the ion signal showed a threshold behavior and an initial rapid rise. Increasing the laser fluence significantly beyond the threshold fluence of 0.20 ± 0.02 J/cm^2, however, did not substantially increase the ion signal. At the same time, the secondary material ejection induced by the recoil pressure expelled more material in the form of particulate matter leading to the depletion of the sample and the clogging of the mass spectrometer orifice. Thus, a fluence just above the threshold value, which also corresponded to a weak phase explosion regime (Chen et al. 2006a), was chosen for the analysis.

Above a certain threshold, the voltage applied to the target did not significantly affect the signal intensity. The threshold voltage for ion detection usually fell in the 50–2500 V range with a polarity that agreed with the charge of the collected ions. Its value depended on the target-orifice distance, the laser fluence, and the type and concentration of the analyte. Typically, ±3.0 kV was applied to the target, which was higher than any observed threshold. Further increasing the voltage was avoided as it increased the possibility of electrical breakdown and instrument failure.

The ion yield dramatically increased as target was moved closer to the inlet orifice. This was demonstrated by measuring the ion yields as a function of target-orifice distance (not shown). However, due to two factors the target could not be moved closer than 2.0 mm to the orifice. First, the dimensions of the laser focusing system presented a physical limitation on the minimum distance between the target and the orifice. Second, due to the high voltage on the target, below 2.0 mm the possibility of electric breakdown increased significantly.

The signal intensity was very sensitive to the radial position of the laser focal spot with respect to the inlet orifice axis. Moving the focal spot off-axis by a fraction of a millimeter dramatically decreased the ion signal.

Changing the orifice temperature between room temperature and 80°C did not significantly affect the analyte ion intensities. At lower temperatures, however, orifice was more susceptible to clogging and close to room temperature abundant water cluster peaks appeared in the low mass region. Higher temperatures resulted in faster drying of the aqueous samples, which led to rapid diminishing of the ion signal with time. Thus, an optimum temperature of 50°C was chosen for these studies as it provided the longest

lasting signal from the sample without clogging the inlet orifice.

3.2 Preingestion analysis of pharmaceuticals

To ascertain the composition of the studied drug formulations and to test the utility of the AP IR-MALDI method, the active ingredients of various pharmaceuticals, administered as gelatin capsule, syrup, tablet and powder, were analyzed using AP IR-MALDI mass spectrometry. The first set of analysis was performed on a thin layer of gel excised from a generic gelatin capsule containing four active ingredients against the common cold and related ailments; acetaminophen (250 mg), dextromethorphan (10 mg), guaifenesin (100 mg), and pseudoephedrine (10 mg). As shown in the Fig. 3, a single scan obtained in one-second (corresponding to 10 laser shots) showed the molecular ion peaks of all four active ingredients. Some of their common fragments were also observed. For example, acetaminophen is observed at *m/z* 152.0705 as a protonated molecular species and at *m/z* 110.0616 as the corresponding fragment due to ketene loss. As it is described by Chen et al., the loss of ketene from acetaminophen has also been found in DESI mass spectra (Chen et al. 2005). Other identified peaks included excipients, for example polyethylene glycol (PEG) used in the formulation of the drug. The signal from PEG is further analyzed in the following section.

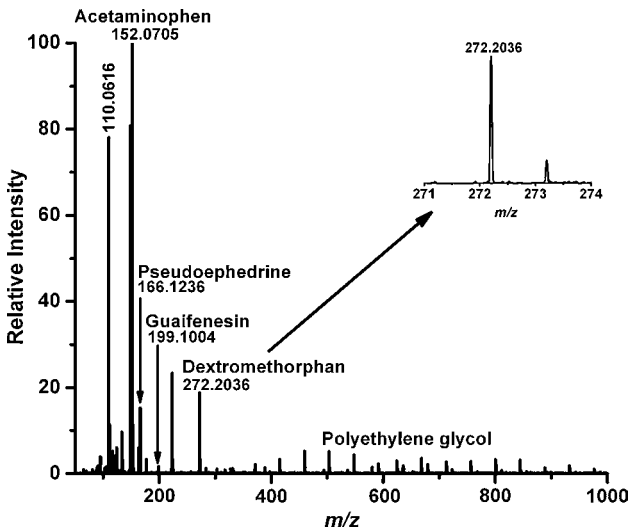

Fig. 3 Single scan mass spectrum of a generic cough medicine formulated as gelatin capsule acquired in 1 second (10 laser shots). It demonstrates the possibility of using AP IR-MALDI for the high-throughput analysis of pharmaceuticals. The molecular ions of all active ingredients (acetaminophen, dextromethorphan, guaifenesin and pseudoephedrine) as well as the oligomers of an excipient (polyethylene glycol) were detected in the mass spectrum. In the inset, the isotope distribution was revealed by zooming in on the dextromethrophan molecular ion (*m/z* 272.2036)

The formulations of the active ingredients with different excipients or the presence of other active ingredients did not affect the analysis by AP IR-MALDI. For example, pseudoephedrine formulated as gel, syrup, solution, tablet and powder produced the same protonated ion at nominal *m/z* 166, and the same fragmentation pattern upon collision activated dissociation. Compared to the wet samples, the positive ion mass spectra of nonwetted tablet/powder samples showed lower intensities for the protonated molecular ions. A few of the drugs, such as ibuprofen, did not produce signal for protonated molecular ions in the positive ion mode. Instead, a fragment ion was observed at *m/z* 161.1328, due to the loss of HCOOH (formic acid).

In the negative ion mode, for ibuprofen the deprotonated molecular ion was observed at *m/z* 205.1271, as expected. The negative ion mode proved to be a useful complementary tool in the detection of compounds that are not easily ionized as protonated species. All of the active ingredients listed in the Table 1, with the formulation and *m/z* values, were detected within a few seconds of analysis per sample. These preliminary results suggest that automated AP IR-MALDI can be used for the high-throughput detection of ingredients in diverse formulations of pharmaceuticals.

3.3 Detection of xenobiotic and endogenous metabolites in urine

Urine is an easily and noninvasively collected biofluid rich in both endogenous and xenobiotic metabolites. The rapid detection of drug metabolites in urine can be challenging due to their low concentrations and interferences from endogenous biomolecules. Two of the major components in urine, water and urea, exhibit strong absorption at the 2.94 μm laser wavelength and thus can act as a matrix for AP IR-MALDI. To determine the role of water in the ionization process of urine samples, it was eliminated through drying and reintroduced. The air-dried urine sample failed to produce any mass spectrum while the sample re-wetted with a few microliters of water produced nearly identical mass spectra to the original. This simple experiment indicated that water acted as a matrix in the mid-infrared laser desorption ionization of the molecular components in urine.

The pharmacokinetics of absorption, distribution, metabolism and excretion (ADME) of a drug molecule is pivotal in drug development (Caldwell et al. 1995). To follow the excretion of xenobiotic compounds, an over-the-counter cough medicine, containing pseudoephedrine (10 mg) and three other active ingredients described previously, was orally administered to a healthy volunteer. Urine samples were collected before and 2.5 h and 24 h after the ingestion of the medication. Pseudoephedrine is a

Table 1 Comparison of measured and calculated monoisotopic *m/z* values for the analyzed active ingredients

Active ingredient	Chemical formula	Monoisotopic mass	Measured *m/z*[a]		Δm (mDa)	Studied formulations
Acetaminophen	$C_8H_9NO_2$	152.0712	152.0705	(+H)	−0.70	Gelatin capsule*, pure analyte, syrup, tablet
Aspirin	$C_9H_8O_4$	181.0501	181.0489	(+H)	−1.20	Powder*
Caffeine	$C_8H_{10}N_4O_2$	195.0882	195.0926	(+H)	4.40	Powder*, tablet
Dextromethorphan	$C_{18}H_{25}NO$	272.2014	272.2036	(+H)	2.20	Gelatin capsule*, syrup
Doxylamine	$C_{17}H_{22}N_2O$	271.1810	271.1737	(+H)	−7.30	Syrup*
Guaifenesin	$C_{10}H_{14}O_4$	199.0970	199.0952	(+H)	−1.80	Gelatin capsule*, syrup
Ibuprofen	$C_{13}H_{18}O_2$	205.1229	205.1271	(−H)	4.20	Tablet*
Ketoprofen	$C_{16}H_{14}O_3$	255.1021	255.0988	(+H)	−3.30	Pure analyte*
Loratadine	$C_{22}H_{23}ClN_2O_2$	383.1526	383.1516	(+H)	−1.00	Pure analyte*, tablet
Melatonin	$C_{13}H_{16}N_2O_2$	233.1290	233.1231	(+H)	−5.90	Pure analyte*
Naphthoquinone	$C_{10}H_6O_2$	159.0446	159.0359	(+H)	−8.70	Pure analyte*
Propranolol	$C_{16}H_{21}NO_2$	260.1650	260.1649	(+H)	−0.10	Pure analyte*
Pseudoephedrine	$C_{10}H_{15}NO$	166.1232	166.1236	(+H)	0.40	Gelatin capsule*, pure analyte, syrup, tablet
Verapamil	$C_{27}H_{38}N_2O_4$	455.2910	455.2910	(+H)	0.00	Pure analyte*

* Formulation of the active ingredient used to obtain the measured *m/z* value

[a] Symbols in parentheses: (+H) indicate protonated and (−H) indicate deprotonated species

common nasal decongestant used for the treatment of common cold and other related aliments. It is known that more than eighty percent of the administered pseudoephedrine is excreted unchanged in the urine within 24 h, peaking at 4 h following its oral administration. Only a small fraction of the pseudoephedrine is metabolized to norpseudoephedrine through N-demethylation (Chester et al. 2004).

Small volumes (3 µl) of the unprocessed urine sample were analyzed directly without drying, extraction or any other sample preparation steps. For the investigation of xenobiotics and endogenous metabolites in the urine, an average of more than 200 mass spectra was collected. The target was continuously rastered to ensure even sampling of the target surface. The mass spectra were further validated by multiple analyses of the same sample as well as by a parallel study on the same individual within two weeks.

In the urine collected after 2.5 h, the protonated pseudoephedrine was detected at *m/z* 166.1239 along with its fragment after OH loss at *m/z* 148.1124. As shown in Fig. 4a, the metabolites for dextromethorphan at *m/z* 272.208, guaifenesin at *m/z* 199.1037 and acetaminophen at *m/z* 152.0696, as well as the excipients such as polyethylene glycol and mannitol/sorbitol (*m/z* 183.0795) were also detected in the urine spectra. Panels b, c and d in Fig. 4 compare the relative intensities of pseudoephedrine peaks at before, and 2.5 h and 24 h following taking the medication, respectively. It is discernable from Fig. 4b that the control urine sample taken before the oral administration of the medication did not contain any peaks for pseudoephedrine. Compared to the 2.5 h level, the urine sample collected at 24 h showed a relative ion intensity reduced by ~84% for pseudoephedrine.

Along with the xenobiotic drug metabolites, many ions related to endogenous compounds were also observed in the urine mass spectrum. The identification of the endogenous metabolites was based on matching the observed monoisotopic mass (within ± Δm 35 mDa), and isotope distribution with those of known metabolites for normal human urine listed in the Human Metabolome Database (http://www.hmdb.ca/ accessed on March 8, 2008) (Wishart et al. 2007). The list of metabolites directly detected by AP IR-MALDI in the urine with their suggested identifications and biological activities are listed in Table 2 (positive ions), and in Table 3 (negative ions). Except for a few noted instances, the reported biological activities of the listed metabolites were obtained from the KEGG (Kyoto Encyclopedia of Genes and Genomes) pathway database (http://www.genome.jp/kegg/pathway.html accessed on March 8, 2008) (Kanehisa and Goto 2000).

The most abundant components in the urine samples were detected both as protonated and as sodiated species. For example, urea, which accounts for half of the total urinary solid, was detected both as *m/z* 61.0318 ($M + H^+$) and *m/z* 83.0161 ($M + Na^+$). The positive ion AP IR-MALDI spectrum of urine showed peaks for diverse chemical species such as amino acids, organic acids, amines, ketones, carbohydrates, steroids, etc. Compared to the positive ion spectra, fewer ions were identified in the negative ion mode, which mainly derived ions from organic acids and amines. A complementary set of metabolites were found in the positive and negative ion spectra.

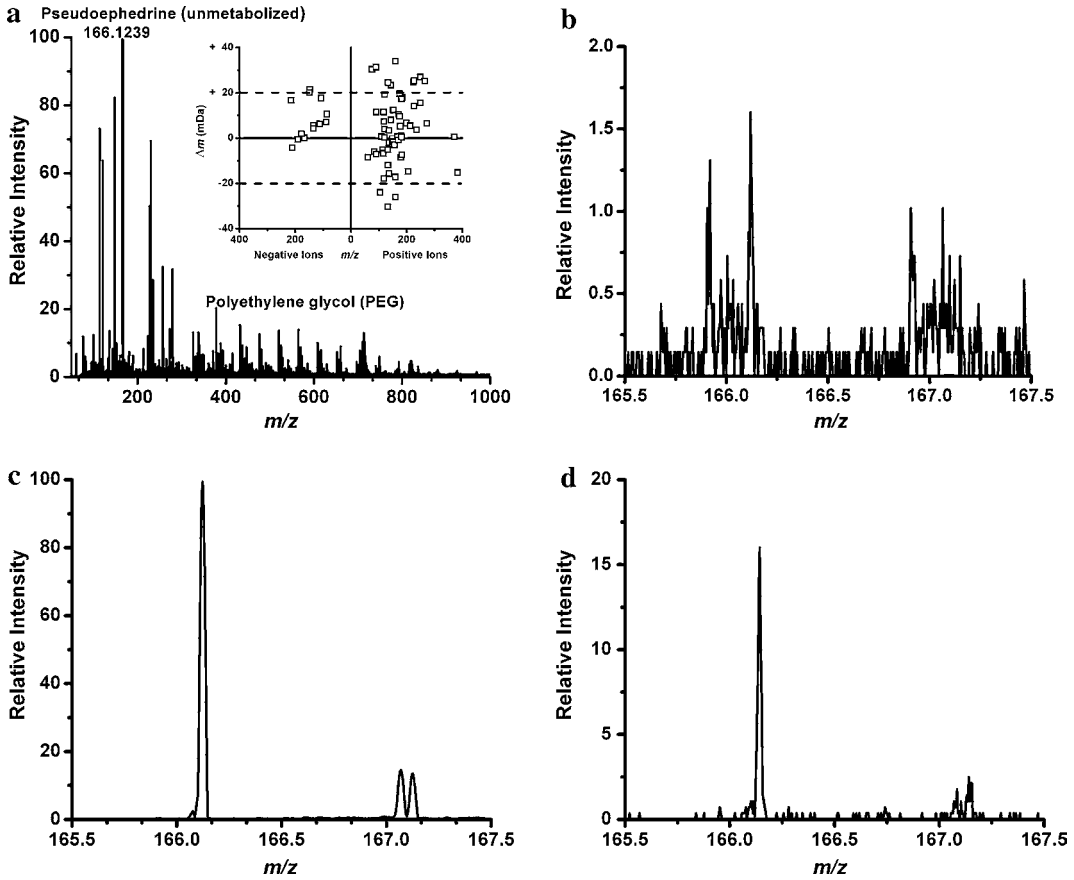

Fig. 4 Typical averaged mass spectra of 3 µl of the urine sample collected (**a**) 2.5 h after drug ingestion clearly shows the molecular ion for unmetabolized pseudoephedrine in the urine as well as peaks related to an excipient, polyethylene glycol (PEG). In the inset the accuracy of the mass measurement, Δm, in mDa units for the metabolites in urine as a function of the theoretical *m/z* value indicates that most species are detected within 20 mDa of the theoretical *m/z* value. Panels (**b**), (**c**) and (**d**) show the mass spectrum in the vicinity of the protonated pseudoephedrine molecule before and 2.5 h and 24 h following the ingestion of the drug, respectively

Some metabolites have close *m/z* values and similar chemical composition. Accurate *m/z* values and isotopic distributions alone might not be sufficient to identify them. For example, the *m/z* 166.1239 ion might correspond to either unmetabolized pseudoephedrine or to hordenine, a phenylethylamine alkaloid found in human urine after consumption of beer brewed using barley (Wishart et al. 2007). Both have the same chemical formula and thus the same monoistopic mass of 165.1154. The *m/z* 166.1239 ion was identified as pseudoephedrine after it had produced a CAD fragmentation pattern identical to pseudoephedrine from the formulated medicine. The CAD spectra for the *m/z* 166.1239 ion from urine, pure analytical standard and medicine formulation are shown in panels (a), (b) and (c) of Fig. 5, respectively. This example shows that AP IR-MALDI combined with tandem mass spectrometry can be used to unambiguously identify detected metabolites. Tandem mass spectrometric analysis was not performed on all detected metabolites, thus, some of the *m/z* values have more than one assignment.

Detecting xenobiotic metabolites originating from pharmaceuticals can help to assess the pharmacological and toxicological effects of drug candidates, while identifying endogenous metabolites might have essential diagnostic applications in the biomedical sciences and in clinical applications. Mass spectrometers have already been successfully used in the diagnosis of many metabolic disorders, e.g., in screening for inborn metabolic disorders in infants (Kuhara 2007; Millington et al. 1990; Wilcken et al. 2003). For example, the more than a dozen amino acids that have been identified in the ~3 µl of urine sample within seconds can be used in gastrointestinal nutritional assessment, and in the diagnosis of metabolic disorders (Brand et al. 1997; Strauss 2004). The detection of amino acids by AP IR-MALDI is faster than any of the classical methods of analysis by specialized assays for each analyte or the simultaneous detection afforded by hyphenated mass spectrometric techniques. With an appropriate internal standard, AP IR-MALDI tandem mass spectrometry might be used as a screening tool for the diagnosis and prognosis

Table 2 Suggested identification of the metabolites detected in the positive ion mass spectra of normal human urine

Metabolite[a]	Chemical Formula	Monoisotopic mass	Measured m/z[c]		Δm (mDa)	Biological activity[b]
Urea	CH_4N_2O	61.0402	61.0318	(+H)	−8.4	Urea cycle and metabolism of amino groups, purine metabolism, pyrimidine metabolism, arginine and proline metabolism, etc.
		83.0221	83.0161	(+Na)	−6.0	
Glycine	$C_2H_5NO_2$	76.0399	76.0703	(+H)	30.4	Bile acid biosynthesis, purine metabolism, glycine, serine and threonine metabolism, lysine degradation, cyanoamino acid metabolism, etc.
Pyruvic acid	$C_3H_4O_3$	89.0239	89.0552	(+H)	31.3	Glycolysis/gluconeogenesis, citrate cycle (TCA cycle), pentose phosphate pathway, pentose and glucuronate interconversions, etc.
Alanine	$C_3H_7NO_2$	90.0555	90.0485	(+H)	−7.0	Alanine and aspartate metabolism, cysteine metabolism, taurine and hypotaurine metabolism, D-alanine metabolism, etc.
Dihydroxyacetone	$C_3H_6O_3$	91.0395	91.0509	(+H)	11.4	Glycerolipid metabolism, methane metabolism
Lactic acid			91.0509	(+H)		Glycolysis/gluconeogenesis, pyruvate metabolism, propanoate metabolism, styrene degradation
Hydroxybutyric acid	$C_4H_8O_3$	105.0552	105.0313	(+H)	−23.9	Propanoate metabolism, in urine during ketosis*
Aminophenol	C_6H_7NO	110.0606	110.0613	(+H)	0.7	Acetaminophen metabolite*
Creatinine	$C_4H_7N_3O$	114.0667	114.0615	(+H)	−5.2	Arginine and proline metabolism
		136.0487	136.0466	(+Na)	−2.1	
Proline	$C_5H_9NO_2$	116.0712	116.0645		−6.7	Arginine and proline metabolism, novobiocin biosynthesis, aminoacyl-tRNA biosynthesis, ABC transporters—general
Dimethylpyruvate	$C_5H_8O_3$	117.0552	117.0666	(+H)	11.4	Valine, leucine and isoleucine biosynthesis, pantothenate and CoA biosynthesis*
Betaine	$C_5H_{11}NO_2$	118.0868	118.0690	(+H)	−17.8	Glycine, serine and threonine metabolism, ABC transporters—general
Valine						Valine, leucine and isoleucine degradation/biosynthesis, propanoate metabolism, pantothenate and CoA biosynthesis, etc.
Guanidoacetic acid	$C_3H_7N_3O_2$	118.0617	118.0690	(+H)	7.3	Precursor of Creatine, *glycine, serine and threonine metabolism, arginine and proline metabolism
Threonine	$C_4H_9NO_3$	120.0661	120.0664	(+H)	0.3	Glycine, serine and threonine metabolism, valine, leucine and isoleucine biosynthesis, porphyrin and chlorophyll metabolism, etc.
3,4-Dihydroxybutyric acid	$C_4H_8O_4$	121.0501	121.0693	(+H)	19.2	Pentose phosphate pathway*
		143.0320	143.0554	(+Na)	23.4	
4-Hydroxystyrene	C_8H_8O	121.0653	121.0693	(+H)	4.0	Phenylpropanoid biosynthesis; metabolite of wines, foods and berries*
		143.0473	143.0554	(+Na)	8.1	
Creatine	$C_4H_9N_3O_2$	132.0773	132.0722	(+H)	−5.1	Glycine, serine and threonine metabolism, arginine and proline metabolism

Table 2 continued

Metabolite[a]	Chemical Formula	Monoisotopic mass	Measured m/z[c]		Δm (mDa)	Biological activity[b]
Leucine	$C_6H_{13}NO_2$	132.1025	132.0722	(+H)	−30.3	Valine, leucine and isoleucine degradation/biosynthesis, aminoacyl-tRNA biosynthesis, ABC transporters—general
Isoleucine						Valine, leucine and isoleucine degradation/biosynthesis, alkaloid biosynthesis II, Aminoacyl-tRNA biosynthesis, etc.
Asparagine	$C_4H_8N_2O_3$	133.0613	133.0858	(+H)	24.5	Alanine and aspartate metabolism, tetracycline biosynthesis, cyanoamino acid metabolism, nitrogen metabolism, etc.
Ureidopropionic acid						Pyrimidine metabolism, beta-alanine metabolism, pantothenate and CoA biosynthesis
Ornithine	$C_5H_{12}N_2O_2$	133.0977	133.0858	(+H)	−11.9	Urea cycle and metabolism of amino groups, arginine and proline metabolism, D-Arginine and D-ornithine metabolism, etc.
Methylcysteine	$C_4H_9NO_2S$	136.0432	136.0466	(+H)	3.4	Garlic metabolite*
Adenine (Vitamin B4)	$C_5H_5N_5$	136.0623	136.0466	(+H)	−15.7	Urea cycle and metabolism of amino groups, purine metabolism
Tyramine	$C_8H_{11}NO$	160.0738	160.1078	(+Na)	34.0	Tyrosine metabolism, alkaloid biosynthesis I, neuroactive ligand-receptor interaction
Glutamine	$C_5H_{10}N_2O_3$	147.0770	147.0744	(+H)	−2.6	Purine metabolism, pyrimidine metabolism, glutamate metabolism, D-glutamine and D-glutamate metabolism, nitrogen metabolism, etc.
Pseudoephedrine fragment	$C_{10}H_{14}$ N	148.1126	148.1124	(+H)	−0.2	Pseudoephedrine metabolite*
Guanine	$C_5H_5N_5O$	152.0572	152.0696	(+H)	12.4	Purine metabolism
Acetaminophen	$C_8H_9NO_2$	152.0712	152.0696	(+H)	−1.6	Acetaminophen metabolite*
Histidine	$C_6H_9N_3O_2$	156.0773	156.0743	(+H)	−3.0	Histidine metabolism, beta-alanine metabolism, aminoacyl-tRNA biosynthesis, ABC transporters-–general
Oenanthic ether	$C_9H_{18}O_2$	159.1385	159.1213	(+H)	−17.2	Human sweat*
Aminooctanoic acid	$C_8H_{17}NO_2$	160.1338	160.1078	(+H)	−26.0	Urine metabolite*
Nicotine	$C_{10}H_{14}N_2$	185.1055	185.1235	(+Na)	18.0	Nicotine metabolite, alkaloid biosynthesis II
Pseudoephedrine	$C_{10}H_{15}NO$	166.1232	166.1239	(+H)	0.7	Pseudoephedrine metabolite*
Hydroxydopamine	$C_8H_{11}NO_3$	170.0817	170.0922	(+H)	10.5	Tyrosine metabolism, amine in human urine
Norepinephrine				(+H)		Tyrosine metabolism, neuroactive ligand-receptor interaction, gap junction
Methylhistidine	$C_7H_{11}N_3O_2$	170.0930	170.0922	(+H)	−0.8	Histidine metabolism
Oxoarginine	$C_6H_{11}N_3O_3$	174.0879	174.0976	(+H)	9.7	Urea cycle and metabolism of amino groups
Arginine	$C_6H_{14}N_4O_2$	175.1195	175.1391	(+H)	19.6	Urea cycle and metabolism of amino groups, arginine and proline metabolism, clavulanic acid biosynthesis, D-Arginine and D-ornithine metabolism, etc.
Ascorbic acid	$C_6H_8O_6$	177.0399	177.0452	(+H)	5.3	Ascorbate and aldarate metabolism, phosphotransferase system (PTS)

Table 2 continued

Metabolite[a]	Chemical Formula	Monoisotopic mass	Measured *m/z*[c]		Δm (mDa)	Biological activity[b]
Cysteinylglycine	$C_5H_{10}N_2O_3S$	179.0490	179.0405	(+H)	−8.5	Glutathione metabolism
Succinoylpyridine	$C_9H_9NO_3$	180.0661	180.0670	(+H)	0.9	Nicotine metabolite*
D-hexose sugar	$C_6H_{12}O_6$	181.0712	181.0717	(+H)	0.5	Urine metabolite*
Tyrosine	$C_9H_{11}NO_3$	182.0817	182.0991	(+H)	17.4	Tyrosine metabolism, phenylalanine, tyrosine and tryptophan biosynthesis, novobiocin biosynthesis, thiamine metabolism, etc.
4-Hydroxy-4-(3-pyridyl)-butanoic acid						
Mannitol/sorbitol	$C_6H_{14}O_6$	183.0869	183.0795		−7.4	Excipient in medicine*
Guaifenesin	$C_{10}H_{14}O_4$	199.0970	199.1037	(+H)	6.7	Guaifenesin metabolite*
Tryptophan	$C_{11}H_{12}N_2O_2$	205.0977	205.0830	(+H)	−14.7	Tryptophan metabolism, Phenylalanine, tyrosine and tryptophan biosynthesis, Indole and ipecac alkaloid biosynthesis, Aminoacyl-tRNA biosynthesis
Vanillactic acid	$C_{10}H_{12}O_5$	213.0763	213.0817	(+H)	5.4	Acidic catecholamine metabolite*
		235.0583	235.0620	(+Na)	3.7	
Cystathionine	$C_7H_{14}N_2O_4S$	223.0753	223.1001	(+H)	24.8	Associated with cystathioninuria, *glycine, serine and threonine metabolism, methionine metabolism
Porphobilinogen	$C_{10}H_{14}N_2O_4$	227.1032	227.1285	(+H)	25.3	Porphyrin and chlorophyll metabolism
		249.0851	249.1120	(+Na)	26.9	
Carnosine	$C_9H_{14}N_4O_3$	227.1144	227.1285	(+H)	14.1	Alanine and aspartate metabolism, histidine metabolism, beta-Alanine metabolism
		249.0964	249.1120	(+Na)	15.6	
Eugenol	$C_{14}H_{16}O_5$	265.1076	265.1328	(+H)	25.2	Food metabolite*
Dextromethorphan	$C_{18}H_{25}NO$	272.2014	272.2080	(+H)	6.6	Dextromethorphan metabolite*
Aldosterone	$C_{21}H_{28}O_5$	383.1834	383.1682	(+Na)	−15.2	C21-Steroid hormone metabolism
Thromboxane B2	$C_{20}H_{34}O_6$	371.2434	371.2440	(+H)	0.6	Arachidonic acid metabolism
6-keto-Prostaglandin F1a	$C_{20}H_{34}O_6$	371.2434	371.2440	(+H)	0.6	Arachidonic acid metabolism

[a] Listed metabolites are obtained from the Human Metabolome Database (http://www.hmdb.ca/ accessed on March 8, 2008) after matching the *m/z* value (within Δm 35 mDa) and the isotopic distribution with the metabolites found in normal human urine

[b] Biological activities are based on the KEGG (Kyoto Encyclopedia of Genes and Genomes) pathway database (http://www.genome.jp/kegg/pathway.html accessed on March 8, 2008) except where marked with * which are based on the Human Metabolome Database (http://www.hmdb.ca/ accessed on March 8, 2008)

[c] Symbols in parentheses, indicate protonated (+H), and sodiated (+Na) species

Table 3 Suggested identification of metabolites detected in the negative ion mass spectrum of normal human urine

Metabolites[a]	Chemical formula	Monoisotopic mass	Measured *m/z*[c]		Δm (10^{-3})	Biological activity[b]
Pyruvic acid	$C_3H_4O_3$	87.0082	86.9976	(−H)	−10.6	Glycolysis/gluconeogenesis, citrate cycle (TCA cycle), pentose phosphate pathway, pentose and glucuronate interconversions, etc.
Lactic acid	$C_3H_6O_3$	89.0239	89.0168	(−H)	−7.1	Glycolysis/gluconeogenesis, pyruvate metabolism, propanoate metabolism, styrene degradation
Dihydroxyacetone						Glycerolipid metabolism, methane metabolism
Cresol	C_7H_8O	107.0497	107.0321	(−H)	−17.6	Toluene and xylene degradation
Creatinine	$C_4H_7N_3O$	112.0511	112.0448	(−H)	−6.3	Arginine and proline metabolism
Hypoxanthine	$C_5H_4N_4O$	135.0307	135.0252	(−H)	−5.5	Purine metabolism
Threonic acid	$C_4H_8O_5$	135.0294	135.0252	(−H)	−4.2	Degradation of ascorbic acid*
Erythronic acid				(−H)		Degradation of ascorbic acid*
Methionine	$C_5H_{11}NO_2S$	148.0432	148.0217	(−H)	−21.5	Methionine metabolism, Aminoacyl-tRNA biosynthesis
Guanine	$C_5H_5N_5O$	150.0416	150.0215	(−H)	−20.1	Purine metabolism
Uric acid	$C_5H_4N_4O_3$	167.0205	167.0204	(−H)	−0.1	Purine metabolism
3-						succinoylpyridine
$C_9H_9NO_3$	178.0504	178.0485	(−H)	−1.9		Nicotine Metabolite*
Citric acid	$C_6H_8O_7$	191.0192	191.0198	(−H)	0.6	Citrate cycle (TCA cycle), Glutamate metabolism, alanine and aspartate metabolism, glyoxylate and dicarboxylate metabolism, etc.
Isocitric acid						
Vanillactic acid	$C_{10}H_{12}O_5$	211.0607	211.0649	(−H)	4.2	Catecholamine metabolite*
Bisnorbiotin	$C_8H_{12}N_2O_3S$	215.0490	215.0323	(−H)	−16.7	Biotin metabolite*

[a] Listed metabolites are obtained from the Human Metabolome Database (http://www.hmdb.ca/ accessed on March 8, 2008) after matching the *m/z* value (within Δm 35 mDa) and the isotopic distribution with the metabolites found in normal human urine

[b] Biological activities are based on the KEGG (Kyoto Encyclopedia of Genes and Genomes) pathway database (http://www.genome.jp/kegg/pathway.html accessed on March 8, 2008) except where marked with * which are based on the Human Metabolome Database (http://www.hmdb.ca/ accessed on March 8, 2008)

[c] Symbols in parentheses indicate deprotonated (−H) species

of disease states. Even with tandem mass spectrometric capability, AP IR-MALDI cannot distinguish between stereoisomers. Online coupling of AP IR-MALDI with chiral separation techniques can be helpful in these cases (McCooeye et al. 2003).

3.4 Potential application in the study of intestinal permeability

Non-invasive intestinal permeability tests using polyethylene glycol (e.g., PEG 400 with MW 280–634) are administered clinically to screen and monitor various gastrointestinal diseases such as the irritable bowel syndrome and Crohn's disease as well as to study gastrointestinal reactions to cytotoxic drugs and food allergens. One form of the intestinal permeability tests includes measuring the urinary excretion of orally administered PEG to give insight into the adsorption and transport of chemicals in the intestine (Bjarnason et al. 1995; Camilleri and Gorman 2007). Although there is an ongoing controversy about the suitability of this test for reliable diagnosis, which we are not addressing here, below we follow the changes upon excretion in the oligomer size distribution of the PEG ingested with cold medication.

PEG oligomers were detected by AP IR-MALDI in both the formulated gelatin capsule and in the urine collected after its oral administration. Without the addition of water, the standard PEG failed to produce any signal, indicating that water played a critical role as the matrix. The PEG ions were observed as a protonated species in the medicine and as sodiated species in the urine. The predominately sodiated PEG peaks in the urine can be explained by the high level of sodium ions excreted in the urine ($\sim$170 mmol per 24 h) (Bingham et al. 1988). For example, the PEG peak at *m/z* 459.2787 in the gelatin capsule is observed as *m/z* 481.2900 in the urine. The difference in *m/z* value between

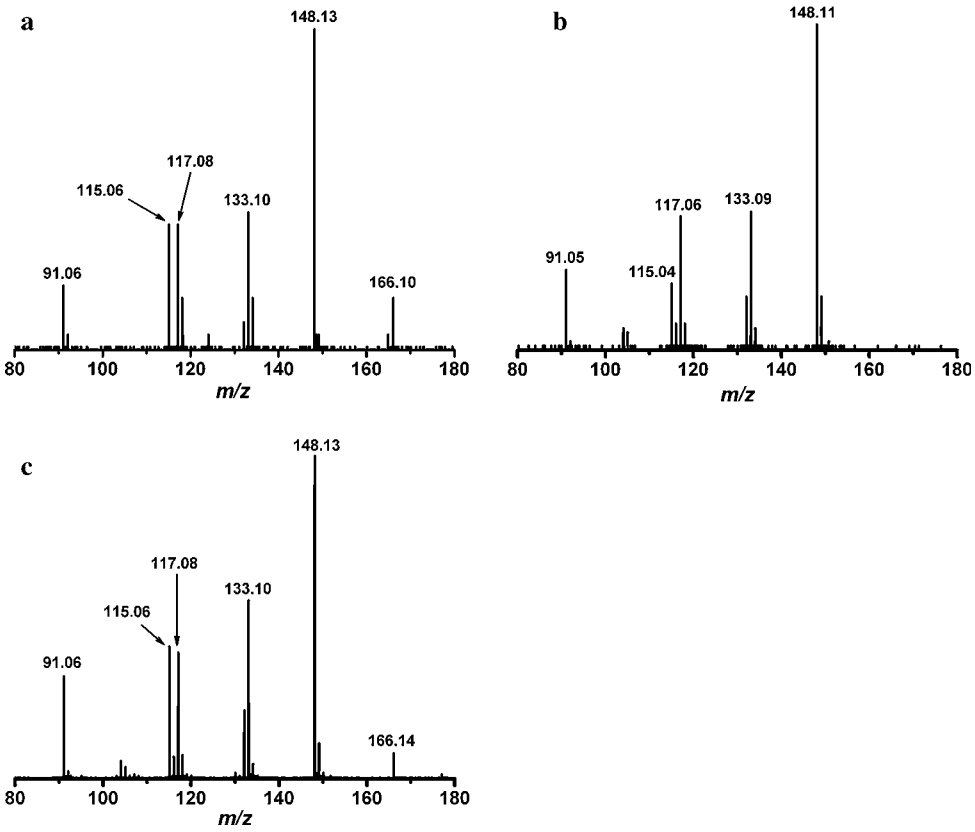

Fig. 5 Fragmentation pattern of the nominal *m/z* 166 ion was obtained by collision activated dissociation to confirm structure of the corresponding metabolite in urine. Tandem mass spectrum of the nominal *m/z* 166 ion is presented in panel (**a**) from urine 2.5 h after the ingestion of the pseudoephedrine containing drug. It produced identical fragments as the tandem mass spectra of (**b**) pure pseudoephedrine analyte and (**c**) pseudoephedrine in the ingested medicine. Similar strategy can be applied to confirm the structure of each unknown metabolite detected in the urine

the two peaks is equal to the mass difference between the protonated and the sodiated species within Δm 29.5 mDa.

Polymers are usually characterized by their repeat units and molecular weight distributions. The molecular weight distribution is described by two average values; the number-average molecular weight, M_{N}, and the weight-average molecular weight, M_{W}, as well as by their polydispersity, *PD*. The average molecular weights and polydispersity are defined as:

$$M_N = \frac{\sum M_i N_i}{\sum N_i}, \tag{1}$$

$$M_W = \frac{\sum M_i^2 N_i}{\sum M_i N_i} \text{ and} \tag{2}$$

$$PD = \frac{M_W}{M_N}, \tag{3}$$

where M_i is the mass of the i-th oligomer and N_i is its abundance represented by the relative intensity in the mass spectrum (Hanton 2001).

The average molecular weights and polydispersity were calculated from the ion intensities and ion masses using equations 1–3. The calculated values for the PEG in the cough medicine were; $M_N = 548$ g/mol, $M_W = 575$ g/mol, $PD = 1.05$. The metabolized PEG excreted in the urine exhibited $M_N = 496$ g/mol, $M_W = 510$ g/mol, $PD = 1.03$. This simple comparison is not intended to actually characterize the intestinal permeability in this case; rather it demonstrates the ability of AP IR-MALDI mass spectrometry to recover oligomer size distribution changes in excreted samples. Further testing of the AP IR-MALDI approach can establish this method for the rapid diagnosis of intestinal permeability. It is worth noting that current techniques require much larger doses of PEG, for example 0.1 g of PEG 400 mixed with 2.5 g of PEG 1000, and the analysis often relies on HPLC analysis (Lahesmaarantala et al. 1991). Establishing AP IR-MALDI for the testing intestinal permeability can substantially reduce the quantity of the administered polymer and significantly shorten the time required for analysis.

4 Concluding remarks

Analysis of biofluids is extensively used to follow metabolic changes. In this communication we demonstrated how the water content of these fluids enables the rapid direct analysis of endogenous metabolites and xenobiotics with AP IR-MALDI mass spectrometry. The wide range of metabolites detected in urine points to diverse applications in metabolism research and to potential clinical uses. For example, the rapid mass spectrometric detection lends itself to large scale stable isotope studies. The minimal sample preparation requirement and extremely fast analysis

time are ideal for high throughput studies and population screening. The analysis at atmospheric pressure outside of the vacuum of the mass spectrometer also provides an opportunity to work with non-traditional samples, e.g., to conduct in vivo pharmacokinetic and diagnostic studies. By coupling the AP IR-MALDI ion source with a translation stage, the analysis method can be used to detect the spatial distributions of metabolites in a tissue (Li et al. 2008). Although the preliminary results presented in this study are encouraging, further improvement is necessary to expand the range of metabolites, and increase both the sensitivity and selectivity. Enhancements in the AP ionization and in the ion collection/transport will increase the sensitivity and possibly the diversity of the collected biomolecules. An automated AP IR-MALDI system with a higher repetition rate laser and the integration of online separation techniques, e.g., ion mobility spectrometry, should enable the swifter detection of a wider variety of biomolecules.

Acknowledgements The authors would like to recognize the financial support from the W. M. Keck Foundation (041904), the U.S. Department of Energy (DEFG02-01ER15129), and the George Washington University Research Enhancement Fund for this work. Modified capillary inlets for the mass spectrometer were kindly provided by D. Kenny of the Waters Co.

References

Balchin, E., Malcolme-Lawes, D. J., Poplett, I. J., et al. (2005). Potential of nuclear quadrupole resonance in pharmaceutical analysis. *Analytical Chemistry, 77*, 3925–3930. doi:10.1021/ac0503658.

Berkenkamp, S., Karas, M., & Hillenkamp, F. (1996). Ice as a matrix for IR-matrix-assisted laser desorption/ionization: Mass spectra from a protein single crystal. *Proceedings of the National Academy of Sciences of the United States of America, 93*, 7003–7007. doi:10.1073/pnas.93.14.7003.

Bingham, S. A., Williams, R., Cole, T. J., Price, C. P., & Cummings, J. H. (1988). Reference values for analytes of 24-h urine collections known to be complete. *Annals of Clinical Biochemistry, 25*, 610–619.

Bjarnason, I., Macpherson, A., & Hollander, D. (1995). Intestinal permeability: An overview. *Gastroenterology, 108*, 1566–1581. doi:10.1016/0016-5085(95)90708-4.

Blanco, M., Coello, J., Iturriaga, H., Maspoch, S., & de la Pezuela, C. (1998). Near-infrared spectroscopy in the pharmaceutical industry. *Analyst (London), 123*, 135R–150R. doi:10.1039/a802531b.

Bowers, L. D. (1997). Analytical advances in detection of performance-enhancing compounds. *Clinical Chemistry, 43*, 1299–1304.

Brand, H. S., Jorning, G. G. A., Chamuleau, R. A. F. M., & Abraham-Inpijn, L. (1997). Effect of a protein-rich meal on urinary and salivary free amino acid concentrations in human subjects. *Clinica Chimica Acta, 264*, 37–47. doi:10.1016/S0009-8981(97)00070-3.

Bunch, J., Clench, M. R., & Richards, D. S. (2004). Determination of pharmaceutical compounds in skin by imaging matrix-assisted laser desorption/ionisation mass spectrometry. *Rapid Communications in Mass Spectrometry, 18*, 3051–3060. doi:10.1002/rcm.1725.

Caldwell, J., Gardner, I., & Swales, N. (1995). An introduction to drug disposition: The basic principles of absorption, distribution, metabolism, and excretion. *Toxicologic Pathology, 23*, 102–114.

Camilleri, M., & Gorman, H. (2007). Intestinal permeability and irritable bowel syndrome. *Neurogastroenterology & Motility, 19*, 545–552. doi:10.1111/j.1365-2982.2007.00925.x.

Chen, Z., Bogaerts, A., & Vertes, A. (2006a). Phase explosion in atmospheric pressure infrared laser ablation from water-rich targets. *Applied Physics Letters, 89*, 041503. doi:10.1063/1.2243961.

Chen, H., Talaty, N. N., Takáts, Z., & Cooks, R. G. (2005). Desorption electrospray ionization mass spectrometry for high-throughput analysis of pharmaceutical samples in the ambient environment. *Analytical Chemistry, 77*, 6915–6927. doi:10.1021/ac050989d.

Chen, H., Venter, A., & Cooks, R. G. (2006b). Extractive electrospray ionization for direct analysis of undiluted urine, milk and other complex mixtures without sample preparation. *Chemical Communications (Cambridge),* 2042–2044. doi:10.1039/b602614a.

Chen, Y., & Vertes, A. (2006). Adjustable fragmentation in laser desorption/ionization from laser-induced silicon microcolumn arrays. *Analytical Chemistry, 78*, 5835–5844. doi:10.1021/ac060405n.

Chen, H. W., Wortmann, A., & Zenobi, R. (2007). Neutral desorption sampling coupled to extractive electrospray ionization mass spectrometry for rapid differentiation of biosamples by metabolomic fingerprinting. *Journal of Mass Spectrometry, 42*, 1123–1135. doi:10.1002/jms.1282.

Chester, N., Mottram, D. R., Reilly, T., & Powell, M. (2004). Elimination of ephedrines in urine following multiple dosing: The consequences for athletes, in relation to doping control. *British Journal of Clinical Pharmacology, 57*, 62–67. doi:10.1046/j.1365-2125.2003.01948.x.

Cody, R. B., Laramee, J. A., & Durst, H. D. (2005). Versatile new ion source for the analysis of materials in open air under ambient conditions. *Analytical Chemistry, 77*, 2297–2302. doi:10.1021/ac050162j.

Cohen, L. H., & Gusev, A. I. (2002). Small molecule analysis by MALDI mass spectrometry. *Analytical and Bioanalytical Chemistry, 373*, 571–586. doi:10.1007/s00216-002-1321-z.

Dettmer, K., Aronov, P. A., & Hammock, B. D. (2007). Mass spectrometry-based metabolomics. *Mass Spectrometry Reviews, 26*, 51–78. doi:10.1002/mas.20108.

Duncan, M. W., Matanovic, G., & Cerpa-Poljak, A. (1993). Quantitative analysis of low molecular weight compounds of biological interest by matrix-assisted laser desorption ionization. *Rapid Communications in Mass Spectrometry, 7*, 1090–1094. doi:10.1002/rcm.1290071207.

Ens, W., Mao, Y., Mayer, F., & Standing, K. G. (1991). Properties of matrix-assisted laser desorption Measurements with a time-to-digital converter. *Rapid Communications in Mass Spectrometry, 5*, 117–123. doi:10.1002/rcm.1290050306.

Glassbrook, N., Beecher, C., & Ryals, J. (2000). Metabolic profiling on the right path. *Nature Biotechnology, 18*, 1157–1161. doi:10.1038/81116.

Go, E. P., Prenni, J. E., Wei, J., et al. (2003). Desorption/ionization on silicon time-of-flight/time-of-flight mass spectrometry. *Analytical Chemistry, 75*, 2504–2506. doi:10.1021/ac026253n.

Guimarães, A. E., Pacheco, M. T. T., Silveira, L., Jr, et al. (2006). Near infrared raman spectroscopy (NIRS): A technique for doping control. *Spectroscopy: An International Journal, 20*, 185–194.

Hanton, S. D. (2001). Mass spectrometry of polymers and polymer surfaces. *Chemical Reviews, 101*, 527–569. doi:10.1021/cr9901081.

Hsieh, Y., Casale, R., Fukuda, E., et al. (2006). Matrix-assisted laser desorption/ionization imaging mass spectrometry for direct

measurement of clozapine in rat brain tissue. *Rapid Communications in Mass Spectrometry, 20*, 965–972. doi:10.1002/rcm.2397.

Kanehisa, M., & Goto, S. (2000). KEGG: Kyoto encyclopedia of genes and genomes. *Nucleic Acids Research, 28*, 27–30. doi:10.1093/nar/28.1.27.

Karas, M., & Hillenkamp, F. (1988). Laser desorption ionization of proteins with molecular masses exceeding 10, 000 Daltons. *Analytical Chemistry, 60*, 2299–2301. doi:10.1021/ac00171a028.

Kauppila, T. J., Wiseman, J. M., Ketola, R. A., et al. (2006). Desorption electrospray ionization mass spectrometry for the analysis of pharmaceuticals and metabolites. *Rapid Communications in Mass Spectrometry, 20*, 387–392. doi:10.1002/rcm.2304.

Kawase, K., Ogawa, Y., Watanabe, Y., & Inoue, H. (2003). Non-destructive terahertz imaging of illicit drugs using spectral fingerprints. *Optics Express, 11*, 2549–2554.

Kostiainen, R., Kotiaho, T., Kuuranne, T., & Auriola, S. (2003). Liquid chromatography/atmospheric pressure ionization-mass spectrometry in drug metabolism studies. *Journal of Mass Spectrometry, 38*, 357–372. doi:10.1002/jms.481.

Kuhara, T. (2007). Noninvasive human metabolome analysis for differential diagnosis of inborn errors of metabolism. *Journal of Chromatography B Analytical Technologies in the Biomedical and Life Sciences, 855*, 42–50. doi:10.1016/j.jchromb.2007.03.031.

Lahesmaarantala, R., Magnusson, K. E., Granfors, K., et al. (1991). Intestinal permeability in patients with Yersinia triggered reactive arthritis. *Annals of the Rheumatic Diseases, 50*, 91–94.

Laiko, V. V., Baldwin, M. A., & Burlingame, A. L. (2000). Atmospheric pressure matrix-assisted laser desorption/ionization mass spectrometry. *Analytical Chemistry, 72*, 652–657. doi:10.1021/ac990998k.

Laiko, V. V., Taranenko, N. I., Berkout, V. D., et al. (2002). Desorption/ionization of biomolecules from aqueous solutions at atmospheric pressure using an infrared laser at 3 [mu]m. *Journal of the American Society for Mass Spectrometry, 13*, 354–361. doi:10.1016/S1044-0305(02)00341-0.

Leuthold, L. A., Mandscheff, J. F., Fathi, M., et al. (2006). Desorption electrospray ionization mass spectrometry: Direct toxicological screening and analysis of illicit Ecstasy tablets. *Rapid Communications in Mass Spectrometry, 20*, 103–110. doi:10.1002/rcm.2280.

Li, Y., Shrestha, B., & Vertes, A. (2007). Atmospheric pressure molecular imaging by infrared MALDI mass spectrometry. *Analytical Chemistry, 79*, 523–532. doi:10.1021/ac061577n.

Li, Y., Shrestha, B., & Vertes, A. (2008). Atmospheric pressure infrared MALDI imaging mass spectrometry for plant metabolomics. *Analytical Chemistry, 80*, 407–420. doi:10.1021/ac701703f.

Lidgard, R., & Duncan, M. W. (1995). Utility of matrix-assisted laser desorption/ionization time-of-flight mass spectrometry for the analysis of low molecular weight compounds. *Rapid Communications in Mass Spectrometry, 9*, 128–132. doi:10.1002/rcm.1290090205.

MacDonald, B. F., & Prebble, K. A. (1993). Some applications of near-infrared reflectance analysis in the pharmaceutical industry. *Journal of Pharmaceutical and Biomedical Analysis, 11*, 1077–1085. doi:10.1016/0731-7085(93)80085-F.

Maher, A. D., Zirah, S. F. M., Holmes, E., & Nicholson, J. K. (2007). Experimental and analytical variation in human urine in 1H NMR spectroscopy-based metabolic phenotyping studies. *Analytical Chemistry, 79*, 5204–5211. doi:10.1021/ac070212f.

McCooeye, M., Ding, L., Gardner, G. J., et al. (2003). Separation and quantitation of the stereoisomers of ephedra alkaloids in natural health products using flow injection-electrospray ionization-high field asymmetric waveform ion mobility spectrometry-mass spectrometry. *Analytical Chemistry, 75*, 2538–2542. doi:10.1021/ac0342020.

Millington, D. S., Kodo, N., Norwood, D. L., & Roe, C. R. (1990). Tandem mass spectrometry: A new method for acylcarnitine profiling with potential for neonatal screening for inborn errors of metabolism. *Journal of Inherited Metabolic Disease, 13*, 321–324. doi:10.1007/BF01799385.

Moreira, A. B., Oliveira, H. P. M., Atvars, T. D. Z., et al. (2005). Direct determination of paracetamol in powdered pharmaceutical samples by fluorescence spectroscopy. *Analytica Chimica Acta, 539*, 257–261. doi:10.1016/j.aca.2005.03.012.

Nemes, P., & Vertes, A. (2007). Laser ablation electrospray ionization for atmospheric pressure, in vivo, and imaging mass spectrometry. *Analytical Chemistry, 79*, 8098–8106. doi:10.1021/ac071181r.

Nicholson, J. K., Connelly, J., Lindon, J. C., & Holmes, E. (2002). Metabonomics: A platform for studying drug toxicity and gene function. *Nature Reviews. Drug Discovery, 1*, 153. doi:10.1038/nrd728.

Niessen, W. M. A. (1999). State-of-the-art in liquid chromatography-mass spectrometry. *Journal of Chromatography A, 856*, 179–197. doi:10.1016/S0021-9673(99)00480-X.

Papac, D. I., & Shahrokh, Z. (2001). Mass spectrometry innovations in drug discovery and development. *Pharmaceutical Research, 18*, 131–145. doi:10.1023/A:1011049231231.

Popchapsky, S. S., & Popchapsky, T. C. (2001). Nuclear magnetic resonance as a tool in drug discovery, metabolism and disposition. *Current Topics in Medicinal Chemistry, 1*, 427–441. doi:10.2174/1568026013394967.

Ratcliffe, L. V., Rutten, F. J. M., Barrett, D. A., et al. (2007). Surface analysis under ambient conditions using plasma-assisted desorption/ionization mass spectrometry. *Analytical Chemistry, 79*, 6094–6101. doi:10.1021/ac070109q.

Reyzer, M. L., Hsieh, Y., Ng, K., Korfmacher, W. A., & Caprioli, R. M. (2003). Direct analysis of drug candidates in tissue by matrix-assisted laser desorption/ionization mass spectrometry. *Journal of Mass Spectrometry, 38*, 1081–1092. doi:10.1002/jms.525.

Siuzdak, G. (1994). The emergence of mass spectrometry in biochemical research. *Proceedings of the National Academy of Sciences of the United States of America, 91*, 11290–11297. doi:10.1073/pnas.91.24.11290.

Smyth, W. F., & Rodriguez, V. (2007). Recent studies of the electrospray ionisation behaviour of selected drugs and their application in capillary electrophoresis-mass spectrometry and liquid chromatography-mass spectrometry. *Journal of Chromatography A, 1159*, 159–174. doi:10.1016/j.chroma.2007.05.003.

Strachan, C. J., Rades, T., Gordon, K. C., & Rantanen, J. (2007). Raman spectroscopy for quantitative analysis of pharmaceutical solids. *The Journal of Pharmacy and Pharmacology, 59*, 179–192. doi:10.1211/jpp.59.2.0005.

Strauss, A. W. (2004). Tandem mass spectrometry in discovery of disorders of the metabolome. *The Journal of Clinical Investigation, 113*, 354–356.

Takats, Z., Cotte-Rodriguez, I., Talaty, N., Chen, H., & Cooks, R. G. (2005). Direct, trace level detection of explosives on ambient surfaces by desorption electrospray ionization mass spectrometry. *Chemical Communications (Cambridge),* 1950–1952.

Takats, Z., Wiseman, J. M., Gologan, B., & Cooks, R. G. (2004). Mass spectrometry sampling under ambient conditions with desorption electrospray ionization. *Science, 306*, 471–473. doi:10.1126/science.1104404.

Tan, P. V., Laiko, V. V., & Doroshenko, V. M. (2004). Atmospheric pressure MALDI with pulsed dynamic focusing for high-efficiency transmission of ions into a mass spectrometer. *Analytical Chemistry, 76*, 2462–2469. doi:10.1021/ac0353177.

Tanaka, K., Ido, H. W. Y., Akita, S., et al. (1988). Protein and polymer analyses up to *m/z* 100 000 by laser ionization time-of-

flight mass spectrometry. *Rapid Communications in Mass Spectrometry, 2*, 151–153. doi:10.1002/rcm.1290020802.

Tang, K., Allman, S. L., Jones, R. B., & Chen, C. H. (1993). Quantitative analysis of biopolymers by matrix-assisted laser desorption. *Analytical Chemistry, 65*, 2164–2166. doi:10.1021/ac00063a041.

Triolo, A., Altamura, M., Cardinali, F., Sisto, A., & Maggi, C. A. (2001). Mass spectrometry and combinatorial chemistry: A short outline. *Journal of Mass Spectrometry, 36*, 1249–1259. doi:10.1002/jms.238.

Wei, J., Buriak, J. M., & Siuzdak, G. (1999). Desorption-ionization mass spectrometry on porous silicon. *Nature, 399*, 243–246. doi:10.1038/20400.

Wei, H., Nolkrantz, K., Powell, D. H., et al. (2004). Electrospray sample deposition for matrix-assisted laser desorption/ionization (MALDI) and atmospheric pressure MALDI mass spectrometry with attomole detection limits. *Rapid Communications in Mass Spectrometry, 18*, 1193–1200. doi:10.1002/rcm.1458.

Wilcken, B., Wiley, V., Hammond, J., & Carpenter, K. (2003). Screening newborns for inborn errors of metabolism by tandem mass spectrometry. *The New England Journal of Medicine, 348*, 2304–2312. doi:10.1056/NEJMoa025225.

Williams, J. P., Patel, V. J., Holland, R., & Scrivens, J. H. (2006). The use of recently described ionisation techniques for the rapid analysis of some common drugs and samples of biological origin. *Rapid Communications in Mass Spectrometry, 20*, 1447–1456. doi:10.1002/rcm.2470.

Wishart, D. S., Tzur, D., Knox, C., et al. (2007). HMDB: The human metabolome database. *Nucleic Acids Research, 35*, D521–D526. doi:10.1093/nar/gkl923.

Wolthers, B. G., & Kraan, G. P. B. (1999). Clinical applications of gas chromatography and gas chromatography-mass spectrometry of steroids. *Journal of Chromatography A, 843*, 247–274. doi:10.1016/S0021-9673(99)00153-3.